Potential energy, relaxation, vibrational dynamics and the boson peak, of hyperquenched glasses

Potential energy, relaxation, vibrational dynamics and the boson peak, of hyperquenched glasses

C Austen Angell[1]**, Yuanzheng Yue**[2]**, Li-Min Wang**[1]**, John R D Copley**[3]**, Steve Borick**[4] **and Stefano Mossa**[5,6]

[1] Department of Chemistry and Biochemistry, Arizona State University, Tempe, AZ 85287, USA
[2] Department of Chemistry, Aalborg University, 9220 Aalborg, Denmark
[3] National Institute of Standards and Technology, Gaithersburg, MD 20899-8562, USA
[4] Scottsdale Community College, Scottsdale, AZ 85256-2626, USA
[5] Laboratoire de Physique Théorique des Liquides, Université Pierre et Marie Curie,
4 Place Jussieu, 5252 Paris Cedex 05, France
[6] Dipartimento di Fisica, INFM Udr and Centre for Statistical Mechanics and Complexity,
Università di Roma 'La Sapienza', Piazzale Aldo Moro 2, I-00185, Roma, Italy

Abstract
We describe a combination of laboratory and simulation studies that give
quantitative information on the energy landscape for glass-forming liquids.
Both types of study focus on the idea of suddenly extracting the thermal energy,
so that the system obtained for subsequent study has the structure, and hence
potential energy, of a liquid at a much higher temperature than the normal glass
temperature T_g. One type of study gives information on the energy that can
be trapped in experimental glasses by hyperquenching, relative to the normal
glass, and on the magnitude of barriers separating basins of attraction on the
landscape. Stepwise annealing studies also give information on the matter
of energy heterogeneity and the question of 'nanogranularity' in liquids near
T_g. The other type of study gives information on the vibrational properties of
a system confined to a given basin, and particularly on how that vibrational
structure changes with the state of configurational excitation of the liquid. A
feature in the low frequency ('boson peak') region of the density of vibrational
states of the normal glass becomes much stronger in the hyperquenched glass.
Qualitatively similar observations are made on heating fragile glass-formers
into the supercooled and stable liquid states. The vibrational dynamics findings
are supported and elucidated by constant pressure molecular dynamics/normal
mode MD/NM simulations/analysis of the densities of states of different
inherent structures of a model fragile liquid (orthoterphenyl (OTP) in the Lewis–
Wahnstrom approximation). These show that, when the temperature is raised
at constant pressure, the total density of states changes in a manner that can be
well represented by a two-Gaussian 'excitation across the centroid', leaving a
third and major Gaussian component unchanging. The low frequency Gaussian
component, which grows with increasing temperature, has a constant peak

frequency of 18 cm^{-1} and is identified with the Boson peak. It is suggested that the latter can serve as a signature for configurational excitations of the ideal glass structure, i.e. the topologically diverse defects of the glassy solid state. The excess *vibrational* heat capacity associated with this generation of low frequency modes with structural excitation is shown to be responsible for about 60% of the jump in heat capacity at T_g, most of the remainder coming from configurational excitation.

1. Introduction

The 'energy landscape' [1–3] has provided an important conceptual route to dissecting the properties of liquids into separate quasi-independent contributions, namely those due to structure and those due to vibrational dynamics. Thus the system is thought of as being characterized by two temperatures, a fictive temperature T_f [4] that relates to potential energy and a real temperature T that relates to kinetic energy. When the two temperatures are the same, the system is a liquid. Otherwise it is a glass.

The possibility of such a dissection depends on the different timescales for vibration and relaxation that characterize viscous liquids. Because of these differences, it is possible to trap the liquid in different states of configurational excitation by cooling at different rates and then to study the effect of trapped structure (or level on the landscape) on the vibrational dynamics of the system. In this paper we use hyperquenching methods (melt spinning of mineral glasses [5–7] and electrospray quenching of molecular glasses [8]) to cool liquids ten million times faster than normal, and thus to trap them in states approaching that of the mode coupling theory T_c, now called the crossover temperature. One objective is to obtain glasses produced on timescales comparable to the most slowly cooled 'computer glasses'. Another is to observe the changes in potential energy, and vibrational dynamics, as a trapped glass finds its way back towards the 'standard' glassy state [8, 9] produced by steady cooling of the liquid at about 0.33 K s^{-1} (20 K min^{-1}). We will need to interpret the finding that, in fact, it never reaches that state unless, first, all memory is removed by returning to the metastable liquid state.

2. Experimental section

Samples for study were prepared using two distinct methods, appropriate to the samples that it was desired to study. Most of the measurements were performed on a room-temperature-stable, micrometre-diameter, fibre material produced from a mineral glass of complex composition (major components in mass% (SiO$_2$ 49.3, Al$_2$O$_3$ 25.6, FeO 11.7, CaO 10.4, MgO 5.5, Na$_2$O 3.9)) which is produced commercially as an insulating material, Rockwool. This material is produced from the molten state at 1700 K by the 'cascade spinner', which consists of a series of rapidly rotating metal discs [7]. Onto the first of these is poured a thin stream of white hot molten material. The discs rotate at approximately 6000 rpm spinning off droplets of liquid, each drawing behind a fine fibre of glass. Melt that does not attach to the first spinning disc is passed to the next and so on until virtually all the melt has been fibred. This product is then sieved (-63 μm) in order to separate the glass droplets from the fine fibres. The cooling rate for the fibres is found to be about 10^6 K s^{-1} [6]. With respect to the volume distribution, the fibres of diameters $d < 4.1$ μm account for 16 vol%, those of $d < 7.7$ μm 50 vol% and those of $d < 12.6$ μm 84 vol%.

From viscosity measurements the precursor liquid state is intermediate in strength, with a $F_{1/2}$ fragility of 0.61, close to that of glycerol, 0.54 [10]. In a simple case like glycerol a $F_{1/2}$ fragility of 0.54 corresponds to an 'm fragility' (or 'steepness index') of 53 [10].

In the second method described in more detail elsewhere [8] a spray of micro-droplets is directed onto the interior surface of a large-sample differential scanning calorimetry (DSC) calorimeter pan, held at liquid nitrogen temperature, using a field of about 10 kV cm^{-1} to electrostatically destabilize the thin stream of liquid emerging from a 200 μm stainless steel capillary tube. The hyperquenched droplets are collected during several distinct bursts. After each burst the surface recovers its initial low temperature. Data for propylene glycol, analysed in [8], show that the cooling rate obtained is between 10^5 and 10^6 K s^{-1}.

To observe the course of the energy evolution during the descent of the landscape at low temperature, we use DSC. We compare the apparent heat capacity during steady upscans of the hyperquenched glass, or some annealed variant of it, with scans of a 'standard glass' obtained by cooling an initially equilibrated liquid sample of the same material into the glassy state at the standard rate, 0.33 K s^{-1}. The latter rate is chosen so that the enthalpy relaxation time at the fictive temperature is 100 s [5, 8, 9]. Details of the protocols used [6] will be given below.

To study the vibrational dynamics of hyperquenched and annealed glasses we use cold neutron scattering time-of-flight measurements carried out using the Disk Chopper Spectrometer at the NIST (National Institute of Standards and Technology) Center for Neutron Research. The measurements were confined to just one of the hyperquenched glasses of this study, namely the 'Rockwool' mineral glass. Typically 15–20 g of material (or 30 g when crystallized) were packed in an 18 mm diameter, 100 mm tall, aluminium can and measurements were performed at room temperature using 4.1 Å incident neutrons. Scattered neutrons were counted in 913 detectors placed 4 m from the sample and their energies were determined by time-of-flight spectroscopy, sorting events into 1000 9 μs time channels. Due to inherent technical limitations, and because of our primary concern with effects in the vicinity of the Boson peak, we concentrate on the low frequency part of the spectrum.

3. Results

In figure 1 we show the upscans of hyperquenched propylene glycol glass compared with the standard scan for the same sample. The latter is run immediately after the initial scan. The area between the two scans corresponds to the energy difference between the sample in the hyperquenched state and the energy of the standard glass which can only be determined when both have been returned to the same state by heating to the upper end of the 'transformation range', about 10% above the onset T_g. The onset T_g corresponds, within 0.5 K, with the fictive temperature of the standard glass, obtained by the usual equal area construction [11]. From these data we can derive the fictive temperature, T_f, of the hyperquenched glass, at which the state of equilibrium of the original liquid was frozen in during the hyperquench. As reported elsewhere [8] this proves to be 15% higher than the standard T_g. Comparable results reported [5, 6] for the hyperquenched silicate glass show that, for this less-fragile glass-former, fictive temperatures as high as 1.25 T_g can be obtained.

The hyperquenched glass can be returned to the standard glass energy in a series of steps, making it possible to obtain a measure of that part of the total frozen-in energy that is released by annealing the hyperquenched glass at a specific temperature for a specific time. For instance, figures 2(a) and (b) show the manner in which the energy lost, during a specific anneal, is determined by scanning a series of samples (a–h) up to the liquid state at 1.1 T_g, after annealing for the temperatures indicated for a specific time. The annealing time is 90 min in figure 2(a) and eight days in figure 2(b). The difference between each of these post-annealing
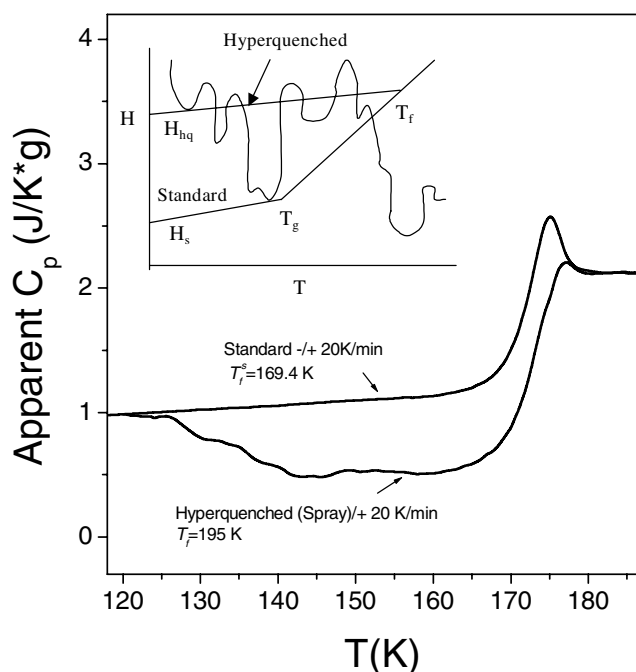
Figure 1. DSC upscans at the standard rate (20 K min^{-1}) of hyperquenched glass of propylene glycol (lower curve) compared with the standard upscan of 'standard' glass (i.e. glass formed by cooling at the standard rate). Integration over the area between the two curves gives the difference in energy between the two glasses. Inset: enthalpy–temperature diagram for glass-formers cooled at different rates, with common representation of energy landscape section superposed.

upscans and the original hyperquenched glass upscan yields, by integration, the amount of energy released during the anneal. The effect of annealing time at a given temperature can be seen by comparing scans such as (h) of figure 2(a) with (f) of figure 2(b). There are several points of great interest in these data that will be discussed in the next section.

Important aspects of the way in which the vibrational dynamics of the glasses in these different trapped states changes with the potential energy of the glass can be revealed by neutron scattering studies [12–15]. The results of our cold neutron inelastic scattering (time-of-flight) measurements are presented in figures 3 and 4 as the function

$$Z(\omega) = A\hbar\omega \frac{(1 - e^{-\hbar\omega/kT})}{(Q_{max}^4 - Q_{min}^4)} \int_{\theta_{min}}^{\theta_{max}} \left(\frac{d^2\sigma}{d\Omega\, dE_f} \right) \sin\theta\, d\theta, \tag{1}$$

where Q and $h\omega$ are the wavevector transfer and energy transfer, respectively, T is the temperature, $(d^2\sigma/d\Omega\, dE_f)$ is the double differential neutron scattering cross section per unit solid angle Ω and final energy E_f, Q_{min} and Q_{max} are ω-dependent extreme values of Q, θ is the scattering angle and A is an arbitrary constant; $Z(\omega)$ may be regarded as a crude representation of an effective vibrational density of states (VDOS), $G(\omega)$, ignoring corrections for effects such as multiphonon and multiple scattering. In our experiments Q_{min} and Q_{max} for elastic scattering (i.e. for scattering with $\omega = 0$) were $\sim$0.3 and $\sim$2.9 Å^{-1}, respectively.

In figure 3 we present data for the hyperquenched glass, and for lower energy states of the same sample produced by annealing. In figure 3(a), the full circles are for the hyperquenched state, the open symbols are for an annealed version of the initial hyperquenched glass which should approximate the 'standard' glass state and the full line is for a 'super-annealed' glass
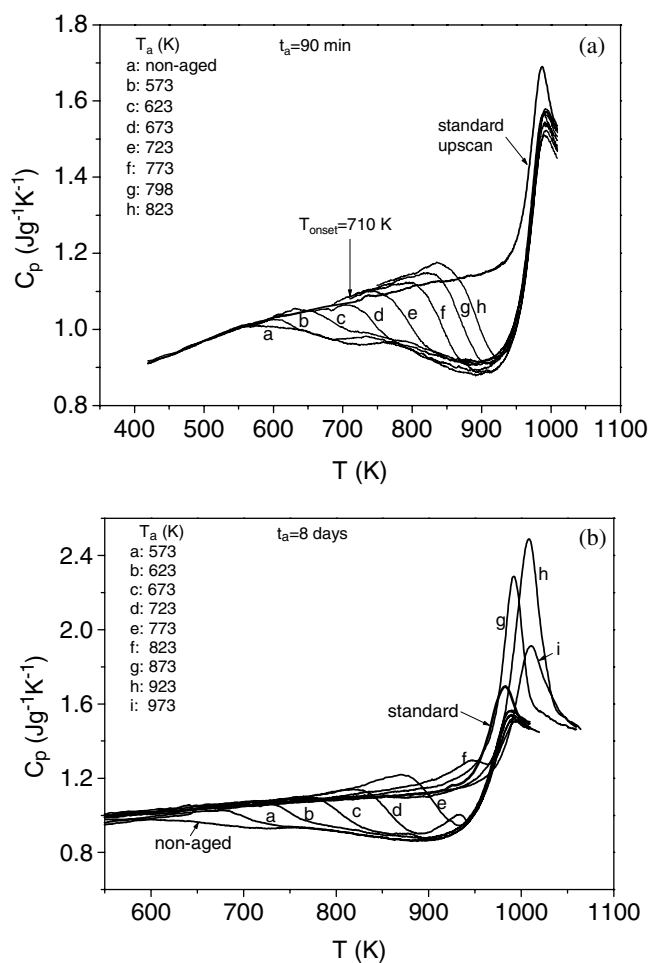
Figure 2. (a) Standard DSC upscans of hyperquenched mineral glasses, after an initial annealing treatment for 90 min at the temperatures designated in the legend. Curve marked 'standard upscan' is for glass cooled from above the transformation range at standard rate of 20 K min^{-1}. It has onset glass temperature and fictive temperature of 944 K. (b) Standard DSC upscans (apparent heat capacities in J g^{-1} K^{-1}) of hyperquenched mineral glasses after an initial annealing treatment for 8 days at each of the temperatures noted in the legend. Note that in this case the selected annealing temperatures extend to temperatures above the standard T_g of 944 K. Note that, for annealing temperatures greater than 823 K, the scans lose the crossover to exothermic responses characteristic of scans (a)–(e) and develop the 'overshoot' usually associated with annealed glasses.

obtained by holding the sample for 21 h at a temperature of 894 K, which is 5.9% below the normal T_g. Finally, the full triangles are for the crystallized material obtained by holding the glass at 1156 K for 150 min.

The excess $Z(\omega)$ at low frequencies of the hyperquenched glass over the value for the annealed glasses (and also the crystal) is the focus of our interest, for reasons that will become especially clear in the final paragraphs of our discussion. Figure 3(b) shows how this excess is emphasized by displaying $Z(\omega)$ for a restricted range of Q values, namely $Q = 0.4$–0.7 Å^{-1}. The physics appears to be most interesting on length scales of $2\pi/Q = 9$–16 Å.

Rockwool, room temperature
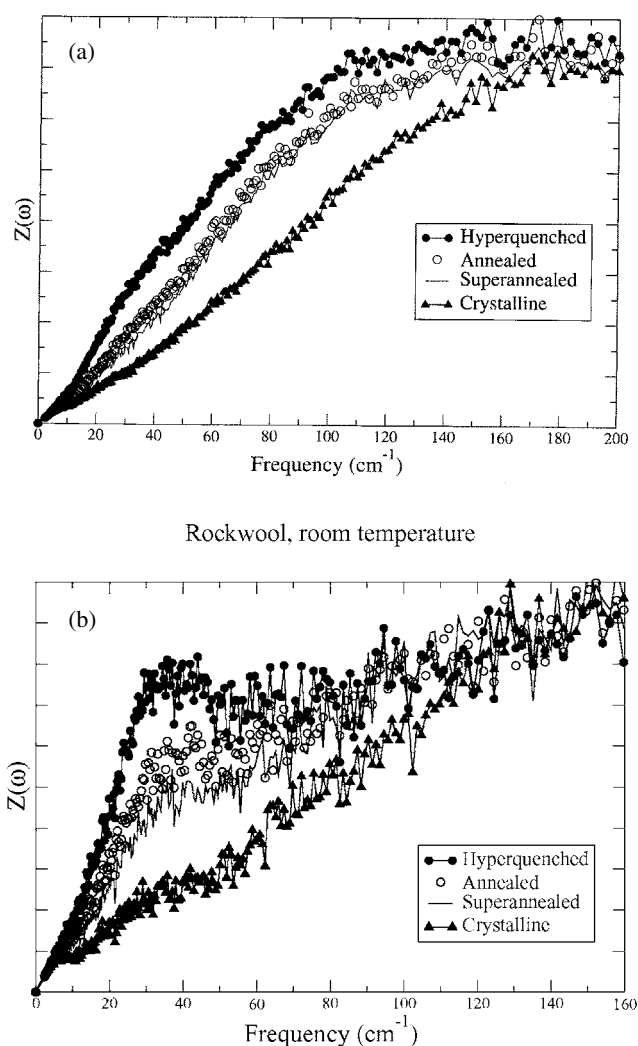
Figure 3. (a) $Z(\omega)$ up to 200 cm^{-1} for the mineral glass in hyperquenched, normal and well-annealed states, and the crystal state, as described in the text. For a monatomic glass corrected for multiple scattering and multiphonon scattering, $Z(\omega)$ approximates the VDOS. (b) $Z(\omega)$ up to 160 cm^{-1} for the same samples as in part (a) except with Q restricted to the range $Q = 0.4$–0.7 Å^{-1}. Note the sharp maximum developed at ~40 cm^{-1} in the case of the hyperquenched glass.

In figure 4 we show $Z(\omega)$ at different temperatures for the fragile aqueous solution glass-former, $Ca(NO_3)_2 \cdot 8H_2O$, which has been well studied by other methods [16]. These plots represent the uncorrected, multicomponent, equivalent of the density of states $G(\omega)$ shown for the elemental glass-former Se by Phillips *et al* [12] in glassy and liquid states. A better analogue might be the DOS for the glassy and liquid states of the fragile molecular glass-former OTP by Wuttke *et al* [15]. The latter authors found that the DOS was independent of temperature for $T < T_g$, but increases at low frequencies for $T > T_g$. The spectra seen in figure 4 are for the glass at 165 K (below T_g of 183 K), at two temperatures 210 and 240 K in the supercooled state, and at ambient temperature, 298 K, where the solution is thermodynamically

$Ca(NO_3)_2 \cdot 8H_2O$
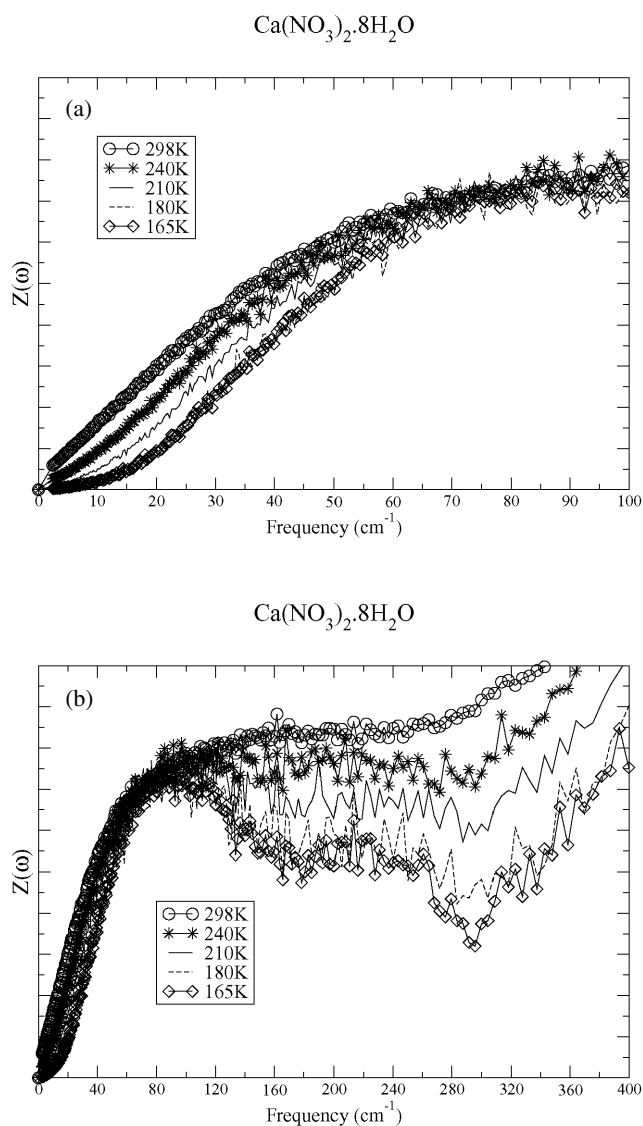
$Ca(NO_3)_2 \cdot 8H_2O$

Figure 4. (a) $Z(\omega)$ up to 100 cm^{-1} for glass, supercooled liquid and stable liquid states of the hydrated salt $Ca(NO_3)_2 \cdot 8H_2O$, as described in the text, showing that excess low frequency modes in high fictive temperature states are restricted to $\omega < 70$ cm^{-1}. Standard T_g is 183 K. (b) $Z(\omega)$ for extended frequency range for the same system and temperatures as in (a), showing the major temperature dependence of DOS in the range 100–400 cm^{-1}.

stable. The sample at 180 K is below the standard glass temperature of 183 K but because of the time taken to set up the experiment and obtain the spectrum it is actually in the ergodic (supercooled liquid) state. It has a spectrum that is indistinguishable from that of the glassy sample at 165 K.

The point to which we address attention in figure 4(a) is the excess $Z(\omega)$ for liquid samples over glassy states at low frequencies, like that of high fictive temperature glasses over low fictive temperature glasses in figure 3. We see the merging of the curves for frequencies

above 70 cm^{-1} in figure 4(a) as the analogue of the crossover in the density of vibrational states of laboratory OTP at 3–4 meV (24–32 cm^{-1}) reported by Wuttke *et al* [15]. A corresponding crossover in the density of states, at ∼40 cm^{-1}, will be seen in another set of DOS data, of much more precisely defined character, obtained from a simulation by one of us [17] to be introduced in the next section, based on the Lewis–Wahnstrom model of OTP [18].

Figure 4(b) shows an extended frequency range for data in the Ca(NO$_3$)$_2$·8H$_2$O system, which shows that something complicated, and distinct from the molecular glass-formers, happens to the DOS at intermediate frequencies. There is a major increase in $Z(\omega)$ with temperature in the frequency range 100–400 cm^{-1}. This effect, which prevents the merging at ∼70 cm^{-1} from becoming an isosbestic point (crossover) as in the molecular OTP case, is probably associated with water hydrogen bonding and solvation structures. While this is a matter of considerable interest in connection with the thermodynamics and fragility of these hydrated melts (because of the extra increases in *vibrational* entropy with fictive temperature that it implies) it will not be considered further in this paper.

4. Discussion

4.1. Relative energy of trapped glassy state, and the trap depth dependence on fictive temperature

First we discuss the relation of the energy trapped in the glass during hyperquenching relative to other quantities such as the energy of fusion and the energy of exciting the liquid to the 'top of the energy landscape' appropriate to the density of the glass. We will compare this with the molar energy of escape from the energy minimum in which it was trapped during the quench. The energy trapped in the glass by hyperquenching is first assessed relative to the energy of the standard glass, by determining the integral over the difference between the two curves of figure 1.

The result is 1.9 kJ mol^{-1}, which is small compared with the energy of fusion of about 12.5 kJ mol^{-1} (based on the value for the 1, 3-propylene glycol, which is crystallizable [19]).

This enthalpy in excess of the standard glass is even smaller relative to the energy needed to excite the system from the normal glass temperature to the top of the system's energy landscape (at the density of the glass). While a precise value for this latter energy is not available (partly because the heat capacity at constant volume is not available over a wide range of temperature) it should be of the order of 20 kJ mol^{-1} according to an argument given in [8]. Thus the range of *glass* potential energies that can be explored by the hyperquenching method is very limited, relative to the range of inherent structure energies that can be explored by computer simulation methods [18, 20]. Notwithstanding this limitation, the fact that hyperquench experiments explore the energetics near the low temperature end of the liquid range where the behaviour is most solid-like, and is also inaccessible to simulation studies at this time, offers special advantages, as we shall see below.

Before considering the exploration of this range in more detail, we need to consider information about the height of the barriers trapping the hyperquenched glass that is available from figure 1. We can estimate this from the temperature, T_{esc}, at which the system starts to relax (i.e. escapes from the trap) during heating at 20 K min^{-1}. From other DSC studies we know this temperature corresponds to the temperature at which the system has an enthalpy relaxation time of 100 s. Assuming the escape is attempted on the inverse vibration frequency timescale, 10^{-14} s, and that the probability of escape is a Boltzmann function of temperature, we obtain the relation

$$\tau = 100 \text{ s} = 10^{-14} \exp(E_{trap}/RT_{esc}) \tag{2}$$
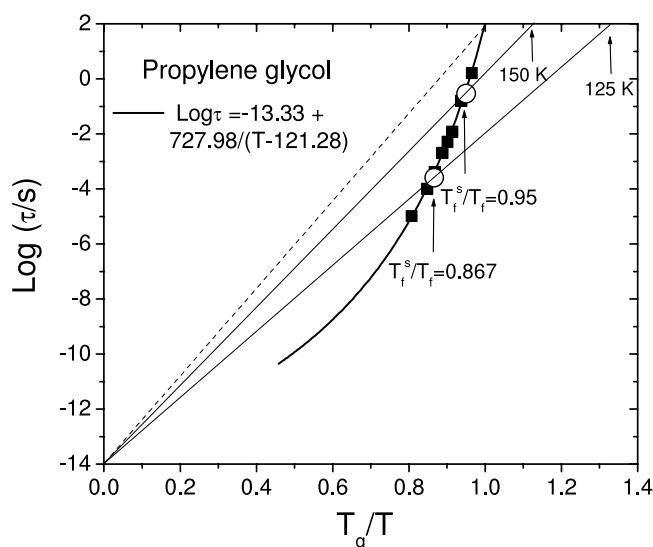
Figure 5. Assessment of the activation energy for relaxation of quenched glasses out of their trap sites, using the scaled fictive temperature, T_f^s/T_f, shown by the open circle marked $T_f^s/T_f = 0.867$. Extrapolation of the straight line construction to $\log \tau = 2$ predicts the temperature at which a glass of this fictive temperature will start to relax during warm-up at the standard DSC heating rate of 20 K min^{-1} (see arrows). The second open circle, $T_f^s/T_f = 0.95$, is for a sample in a sealed DSC pan, quenched (at much lower dT/dt) by dropping into liquid nitrogen (see [8]).

which yields the value $E_{trap} = 39.9$ kJ mol^{-1}, when $T_{esc} = 125$ K is substituted. Since this barrier height, expressed in molar units, is considerably greater than the height of the energy landscape given above, also in molar units, there is clearly some problem of interpretation.

We therefore point out that our estimate of the trap depth is consistent with the estimate of the true activation energy for relaxation in viscous liquids suggested by Dyre [21]. It is also consistent with observations on the ionic conductivity of glasses that exhibit some degree of decoupling of conduction modes from viscous flow modes [22]. This activation energy is the one obtained from the slope of the Arrhenius straight line connecting the point of interest on the log(relaxation time) versus inverse temperature plot, to the attempt frequency, 10^{-14} s (as noted above). That the equation (2) activation energy is consistent with these considerations is seen by taking the relaxation time at the fictive temperature of the hyperquenched glass (obtained in the manner described in [6] and [8]), and connecting it to the 10^{-14} s point at $1/T = 0$. The activation energy obtained from the slope of this line is 40.0 kJ mol^{-1}, essentially the same as from the analysis of equation (2). The construction is shown in figure 5. Its support of the value obtained from equation (2) is seen most clearly from the fact that the extrapolation of the straight line to lower temperatures, to the value $\tau = 100$ s, yields the temperature 125 K. This temperature is almost the same as that used in equation (2) at which relaxation is seen to begin, during the initial upscan at 20 K min^{-1} (figure 1).

The problem of interpretation of these trap depth values will be dealt with elsewhere. We point out, however, that, according to the construction used above, the activation energy for relaxation will be larger when $T_f = T_g$ (standard). At T_g, $E_{esc} = 52$ kJ mol^{-1}. We note also that, by this construction, the activation energy, i.e. trap depth, at T_g will be universal, at $37RT_g$, so long as the pre-exponent remains 10^{-14} s.

It is interesting to compare these trap depth values with the activation energy for diffusion of H_2O molecules in ice, a single-particle process. The activation energy is 58.5 kJ mol^{-1} [23],

which is somewhat in excess of the sublimation energy (51 kJ mol^{-1} [24]). The activation energy for a number of other relaxation processes in ice has the same value [23]. Water, like PG, has two OH groups per molecule.

4.2. Stepwise descent of the landscape, and the possibility of 'nanogranularity' in glass

In figure 1 we have seen the way in which the energy difference between the hyperquenched glass and the normal glass may be manifested in one continuous scan. An opposite extreme can be imagined in which the energy difference is manifested and recorded during long observation at a single temperature. The temperature would be raised suddenly to a temperature of, say, 140 K (somewhat above the Kauzmann temperature of 116 K) and then the release of energy monitored isothermally. One might imagine that, in such an experiment, all the potential energy states usually observed during decrease of temperature from the fictive temperature of the hyperquenched glass to the normal glass temperature could be observed as a function of time alone.

The problem with such a putative experiment is not only that the time required to complete the observation would become excessively long (10^{25} s to relax ($1/e$)th of the way to the equilibrium state, according to the parameters of the well known Vogel–Fulcher–Tammann equation for the most probable relaxation time, noted in figure 6), but that both the initial jump and the initial recording of relaxation would have to be made extremely rapidly because (according to the activation energy determined in the previous section) the initial relaxation would occur on a timescale of 10^{-6} s. A compromise experimental protocol is that used in obtaining figure 2, in which the isothermal annealing is carried out in a series of stages. In each stage, annealing is allowed to occur for a fixed period of time at a succession of temperatures. Because the DSC is not well suited for detecting the small energy releases directly, such measurements are most accurately performed by carrying out an upscan, at the standard rate, at the end of each annealing period. The effect of the anneal is then obtained from the difference between the post-anneal scan and the scan on a sample which has not been annealed at all.

Because this protocol requires a separate sample for each anneal, it is best carried out on a system for which a large amount of hyperquenched material is available. Thus we use the hyperquenched mineral glass to record the annealing behaviour. Figure 2 includes the scan for a standard glass, formed by cooling the sample from the supercooled liquid to the glassy state at the standard 0.33 K s^{-1}(20 K min^{-1}). It is in the comparison of the results of the hyperquenched glass series with the standard glass that this series reveals its most interesting aspect, discussed below.

An alternative to the above protocol is available. This is to choose a fixed annealing temperature, and anneal for a series of different times. Then the fraction of total trapped energy that is released during each anneal can be obtained. Such a series, which also requires a number of identical samples, has been shown already in [6]. In that work, a plot of the fraction of the trapped energy released versus log (time of anneal) demonstrated the non-exponential nature of the relaxation process:

$$\Phi(t) = \Phi_0 \exp -(t/\tau)^\beta \qquad (3)$$

and allowed a stretching exponent β to be determined. The stretching exponent obtained is very small, 0.16, relative to those determined in experiments in the linear response regime (and to that expected, $\sim$0.7, from the approximate correlation of β with the fragility of the glass-former [10]). The difference is a manifestation of the non-linear nature of the relaxation in systems far from equilibrium. The non-linearity causes the relaxation of the hyperquenched glass to be much faster than that of an equilibrated glass at the same temperature (as if the glass
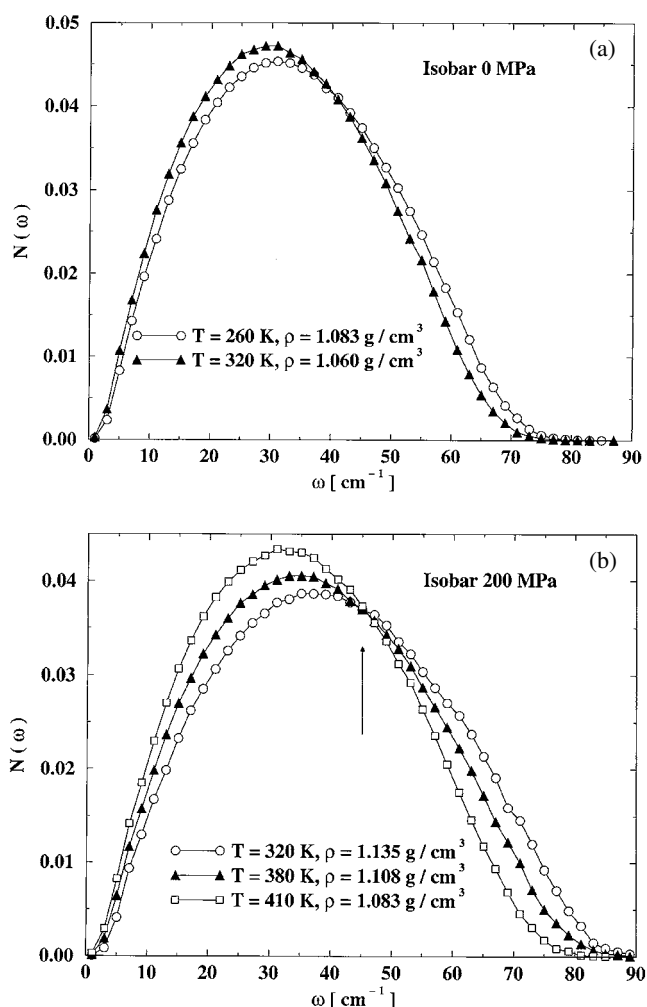
Figure 6. The VDOS for the inherent structures of OTP, in the Lewis–Wahnstrom model, obtained by steepest descent quenching of structures equilibrated at the designated temperatures (a) at 0.1 MPa (1 atm) and (b) at 200 MPa. Note the isosbestic point at $\sim$40 cm^{-1}. The model has no internal degrees of freedom.

is aware of the excess free volume, or entropy, that it possesses). The faster relaxation at short times makes the relaxation look more non-exponential than the linear process actually is.

Returning to the data of figure 2, we note the manner in which annealing at each temperature relaxes out a well defined portion of the total trapped energy, leaving the kinetics of relaxation of the remaining trapped energy completely unaffected. The manner in which the upscans of the samples that were subject to higher temperature anneals, abruptly crossover from a position which is endothermic with respect to the standard glass to one which is strongly exothermic, is quite striking. See, e.g., curve h in figure 2(a). Since Richert [25] has made a strong case for the heterogeneity of relaxation as the source of its non-exponential character, and since the heterogeneity is evidently spatial in character near T_g [26–28], the figure 2 demonstration that the relaxation process is also *energetically* heterogeneous lends credence

to the 'nanogranularity' concept of liquids near T_g. By this we mean the notion that there are independent micro-regions in the glass which are widely distributed in size (and local density) and stable in dimension. That they are stable in dimensions is suggested by the finding, detailed elsewhere [29], that once the apparent heat capacity becomes higher than that of the standard glass, the properties of the glass *up to this temperature*, become reproducible to cycling in temperature. The introduction of probes of local structure (e.g. cobalt ions [30]) into the parent oxide glass could make possible the demonstration that the structures of these micro-regions also becomes stable on annealing to this temperature.

Figure 2 shows that the fast relaxing micro-regions can achieve states that are of low energy relative to the rest of the glass (the total energy of which remains above that of the standard glass) and then can re-absorb that energy during heating at what looks like a mini glass transition. This behaviour cannot be produced by annealing of the standard glass at the same temperature so it, and the annealing pre-peak (or 'shadow' glass transition) that it produces, requires the structure of the unrelaxed portion of the hyperquenched glass for its manifestation (vault effect [31]?). Elsewhere [32], two of us have argued that this is the likely source of the weak endothermic rise in heat capacity observed in annealed forms of amorphous water formed by highly non-equilibrium processes. The endotherm has long been ascribed to a standard glass transition, which is now in question.

The existence of independent micro-regions is also suggested by energy landscape considerations, as follows. A system at constant volume has a unique energy landscape that is fixed by the intermolecular potentials for the particles of the system. In configuration space the system is represented by a point that moves on this surface. The point can only move in one direction at one time. However, figure 2 (and its counterpart in which time is varied at fixed temperature [7]) show that, for partially annealed glasses, the direction in which the energy changes with time during annealing, relative to a standard glass, depends on the timescale on which it is observed. Fast parts of the system increase in energy while slow parts decrease in energy, relatively.

In the real space interpretation, one could argue that the independent nanograins can have different properties, fast parts (perhaps the smallest grains) behaving like *homogeneous* systems of high volume and enthalpy, while slow parts behave like *homogeneous* systems of low volume and enthalpy. While this may sound like an 'ensemble of landscapes', Stillinger (private communication) points out that it is better regarded as an ensemble of 'projections onto lower dimensions of the single higher-dimensional landscape that must encompass the full many-body behaviour of the system of interest'. It is such complexity that is responsible for the fact (illustrated adequately by figures 2(a) and (b), and long known in glass science) that a glass formed by some arbitrary path cannot fully recover the state of the standard glass unless it is first brought into a state of complete internal equilibrium. This means it must first be heated above the glass transformation range, and then cooled to below T_g at the standard rate. (A glass fully equilibrated by annealing long enough at a temperature below the standard T_g will have a lower total energy than the standard.)

The real space picture evoked above has much in common with the 'mosaic' model used by Xia and Wolynes [33] who described the glass transition as a 'random first-order' phase transition.

It should be noted that the above amounts to an attempt to put into microscopic terms what is usually described by phenomenological models such as the Tool–Narayanaswamy–Moynihan [34], Kovacs–Aklonis–Hutchinson–Ramos [35] and Scherer–Hodge [36] models. All of these models contain parameters representing the non-exponentiality of relaxation and non-linearity of relaxation. Each model is capable of predicting the crossover phenomenon, and also the occurrence of the annealing pre-peak [37], but none provides a microscopic account

of the source of the non-exponentiality, and only the Scherer–Hodge model accounts for the origin of non-linear behaviour.

4.3. Vibrational characteristics of glasses in different states of configurational excitation

In this section we discuss a further manifestation of the different structures of hyperquenched and annealed glasses. This is the redistribution of frequencies in the VDOS such as to favour, in high fictive temperature glasses, frequencies near the Boson peak frequency [38], $10^{12.2}$ Hz ($\sim$50 cm^{-1}) [38, 39] or $\sim$30 cm^{-1}, as seen in figures 3 and 4. The Boson *peak* was originally identified from light scattering data [39] and the intensity of scattering is found to relate to the total density of states $G(\omega)_{tot}$ as $G(\omega)_{tot}/\omega^2$ [39]. Division of $Z(\omega)$ in figure 3(a) by ω^2 would certainly emphasize the excess of the $Z(\omega)$ of the hyperquenched glass over that of the standard glass, so one would say that the Boson peak has been greatly enhanced in the hyperquenched glass. In liquids the Boson peak is obscured by increased quasielastic scattering so investigation of glasses in which the high temperature structure is retained but the quasielastic scattering is suppressed—as in hyperquenched glasses—should be a good way to investigate the Boson peak.

The low frequency vibrational spectra of glasses with different quench histories have been studied before. These studies, by Suck [12, 13], have been made on metallic glass-formers in which the fragilities are now known [40] to be significantly less than those of the present system. The findings of Suck and co-workers were qualitatively similar for the different glasses. Each of the hyperquenched states had an excess $G(\omega)$ at low frequencies, and diminished $G(\omega)$ around the Debye frequency, relative to the spectrum for the same glass after annealing. These workers utilized quenching rates of the same magnitude as ours (obtained by melt spinning onto cold rotating metal drums). However the DOS effects were quite small relative to those seen in figure 3, and more in line with those reported by Vollmayr and Kob [41] for simulated binary LJ glasses (the potentials for which were originally modelled on the Ni–P metallic glass-former). The possibility of a distinct maximum emerging in the 'restricted Q density of states', seen in figure 3(b), has not arisen in previous studies. This enhanced feature is worthy of further study for the additional information on the nature of the Boson peak it may provide.

It will be interesting to see how general such findings might be in silicate glasses. Since successful computer simulation studies of silicate glass systems have been made by a number of workers [42–45], it is reasonable to hope that studies of inherent structure densities of states, in systems of different compositions, might help clarify what sort of modes are involved. The suggestion of the present work is that there is a distinct configurational excitation that involves structures in which low frequency modes, presumably with transverse character, are generated. The simplest description of this source of Boson peak oscillation would be that of 'resonance modes' that accompany defects with the character of interstitials in crystals [46]. This has been the suggestion of Granato [47] in advancing his interstitialcy theory of liquids. While Granato's description seems too simple to satisfy the requirements of liquid theory, some topologically diverse form of interstitial excitation, the spectral signature of which would be Gaussian in form as seen below, may indeed eventually prove adequate to describe the observed phenomena.

In this respect the observations made on a model of the fragile glass-former orthoterphenyl (OTP) [17, 18] seem relevant. Before introducing these, however, we must correlate the observations of figure 4 with those of experimental OTP in order to suggest a certain generality for the simple picture to be presented. We earlier noted the similarity of the closing of the excess $Z(\omega)$ domain in Ca(NO$_3$)$_2$·8H$_2$O data of figure 4(a) with the crossing point at $\sim$32 cm^{-1} observed by Wuttke *et al* [15] for the DOS of glassy and liquid OTP. Wuttke *et al* [15] paid little attention to their observation, on the basis that the DOS can 'depend on

temperature only if there are deviations from harmonicity'. However we see their crossing point reproduced below in the DOS of inherent structures of the model OTP, where certainly more than anharmonicity is involved.

In [17], Mossa *et al* show the DOS for inherent structures of OTP explored by the system at three different temperatures, at a series of fixed densities. These were obtained from NM analysis of the inherent structures. They noted the presence of an isosbestic point at 40–45 cm^{-1}. As found by Kob *et al* [48] and Sastry [49] for the mixed Lennard-Jones model, and by Mossa *et al* for OTP [17] high temperatures favour higher frequencies for systems held at constant volume. However, when the volume is adjusted to keep the pressure constant, as happens in most experiments, the reverse behaviour is found [50], as seen also in figures 6. The isosbestic point remains, unchanged in frequency, as shown in figure 6(b).

In figure 7 we show that each of these total DOSs can be well represented by a sum of three Gaussian functions. An interesting observation is made. The centre Gaussian of each DOS, which has the largest area of the three components, is invariant with change in temperature. The differences responsible for the isosbestic point come from the compensating changes occurring in the high and low frequency components. This is the same phenomenon that has been reported recently for the O–D overtone vibrations in water [51] and some time earlier [52, 53] for the overtone O–H stretching mode in deuterated water. A related phenomenon seen in simulated water in the rigid molecule ST2 potential [54] was called 'exciting across the centroid' by Rahman and Stillinger [54], and this seems a very appropriate description for the present observation. The system behaves as if molecules in some Gaussian distribution of strained sites snap into some rearranged group whose low frequency vibrational modes are also distributed in Gaussian form. (A simple two-Gaussian 'strained site' model, with predictive qualities, based on these observations will be described elsewhere [55].) The peak frequency of the low energy Gaussian is 18 cm^{-1}, independent of temperature, while the high energy component has a peak frequency that decreases with increase in temperature.

The peak frequency of the lower energy Gaussian is typical of the Boson peak frequency, and its increase in intensity with decreasing temperature is comparable to that seen in figure 3. Since the two cases have in common that they are properties of systems trapped in high energy configurations and studied at low temperatures, there are good reasons to see them as the same phenomenon. In view of the interest in resolving the nature and origin of the Boson peak, it would seem that studies of hyperquenched inorganic glasses of simpler constitution than the present case should be rewarding. Likewise, DOS studies and 'restricted Q DOS' studies of simulated glasses of different potentials, particularly including simple silicates, are obvious targets for future study. It is possible that these observations will prove consistent with, and provide spectroscopic signatures for, the Gaussian trap models for glassy systems that are currently being discussed in the literature [56, 57].

Before leaving the subject of the inherent structure densities of states seen in figure 6 it is important to take note of the manner in which they permit us to assess the vibrational contributions to the excess properties of the supercooled liquid. While details will be given elsewhere [55], we may summarize the essential findings here.

The entropy-rich low frequency modes generated with increasing temperature (figure 7(b)) provide a large part of the excess entropy of the liquid over crystal (or glass) as the system temperature rises above T_g. They are therefore responsible for much of the jump in heat capacity seen at the glass transition. In the present case this jump in heat capacity, measured at 380 K, is found to be 61 J mol^{-1} K^{-1} (experimental value ΔC_p at 380 K = 68 J mol^{-1} K^{-1}) and of this, a full 60% originates in the change of VDOS with temperature. This increase in vibrational entropy with increasing temperature becomes an important part of the thermodynamic drive for the system to reach the 'top of the landscape', as foreseen in 1976 by Goldstein [58], and
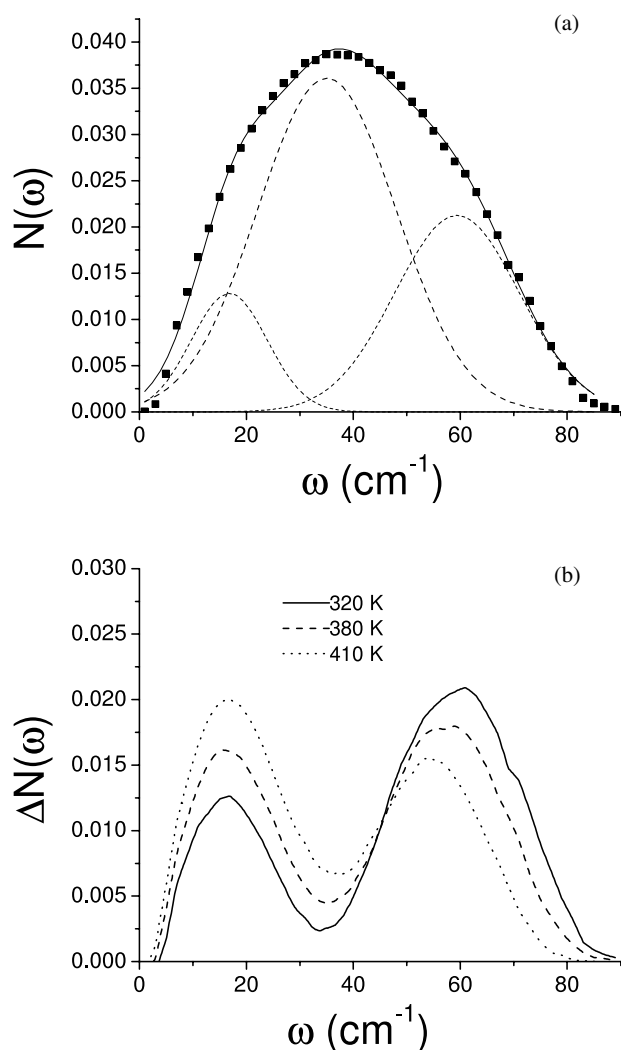
Figure 7. (a) Gaussian decomposition of the 320 K, 200 MPa DOS of figure 6, showing the temperature-independent central component by a broken curve and the match of the total DOS to the three Gaussian representations by a full curve. (b) The three DOS of figure 6(b) after subtraction of the common central component. Excitation of the structure, by increasing temperature at constant pressure, is seen to be associated with transfer of oscillators from the high temperature Gaussian component to the low temperature Gaussian component, which is called 'excitation across the centroid' [53]. Note that the low frequency component has a peak frequency that is independent of temperature. This frequency, ~ 18 cm^{-1}, is typical of the Boson peak.

as recently emphasized in [59]. It therefore is deeply involved in determining the fragility of the liquid state.

The behaviour of OTP (fragile) makes an interesting contrast with that of mixed LJ [41] which, as argued elsewhere [60], is a relatively strong liquid. It also contrasts with that of the laboratory metallic glass PdSiP [14], which is known to be a rather strong liquid [40]. In these, the DOS changes only weakly with fictive temperature. The contrast is even stronger with the behaviour of the *same* system, OTP, under *constant volume* conditions. There [17], behaviour opposite to that seen in figure 6 is encountered: increase of temperature depresses

the low (boson peak) frequency component of the DOS and enhances *higher* frequencies, while preserving an isosbestic point at the same point as in figure 6[7]. It is on record that liquids that are highly fragile according to normal (constant pressure) measurements, appear much less fragile when studied at constant volume. A large diminution was documented recently for the ionic glassformer 'CKN' [61]. Clearly, then, a proper understanding of the boson peak is the key to understanding important parts of the viscous liquid problem.

5. Concluding remarks

How to relate the excitations inferred here (from the low frequency build-up in the DOS) to the evidence for energetic heterogeneity obtained from the anneal-and-scan studies is an unanswered problem at this time. Are the configurational changes involved in the 'excitations across the centroid', which are apparently involved in the boson peak, located in the interiors of the nanodomains or do they form part of their boundaries? Hopefully this and other questions arising from this work will find their answers in follow-up studies on hyperquenched glasses from other carefully chosen systems. It is clear that a much wider range of quenched-in structures can be investigated by computer simulation than by experiment, and since more simply constituted systems can be vitrified by simulation, it must be expected that it is from this quarter that the most rapid progress will be made. On the other hand, it is not clear that simulations can be conducted in a low enough temperature range for the non-exponentiality needed to show the phenomena of figure 2 to have developed.

References

[1] Goldstein M 1969 *J. Chem. Phys.* **51** 3728
[2] Stillinger F H and Weber T A 1984 *Science* **228** 983
     Stillinger F H 1995 *Science* **267** 1935
[3] Sastry S, Debenedetti P G and Stillinger F H 1998 *Nature* **393** 554–7
[4] Tool A Q 1946 *J. Am. Ceram. Soc.* **29** 240
[5] Yue Y-Z, Christiansen J deC and Jensen S L 2002 *Chem. Phys. Lett.* **20** 357
[6] Yue Y-Z, Jensen S L and Christiansen J deC 2002 *Appl. Phys. Lett.* **81** 2983

[7] In this respect there is a conflict with the behaviour of the soft sphere system studied by Parisi [62, 63] at constant volume. Parisi found that increase of temperature caused changes to the DOS which were superficially like those for OTP at constant volume but with a slight excess at low frequencies. Thus where the fragile liquid OTP at constant volume has a Boson peak that decreases in strength with increasing temperature, mixed soft spheres behave weakly in the opposite fashion. Indeed, the presence of large system size effects in the soft sphere system (studied at constant volume) [64], and pronounced 'boson dips' [38] in the self part of the density autocorrelation function of the 2D mixed soft sphere system [65, 66] (which are amplified by system size effects as in [38] figure 26, for SiO_2), suggests that the mixed soft sphere system is not at all a fragile liquid, as unexpected as this might seem at first sight.

[7]   Axten C W, Bauer J M, Boymel P M, Copham J D, Cunningham R N, Kamstrup O, Koenig A, Konzen J L, Ohberg I, Roe C, Sacks J, Singh T M and Wolf W 1991-93 *Man-Made Vitreous Fibers: Nomenclature, Chemical and Physical Properties* ed W Easters (Stamford, CT: Thermal Insulation Manufacturers Association (TIMA Inc.)) p 17

[8]   Wang L-M, Borick S and Angell C A *Phys. Rev.* B submitted

[9]   Velikov V, Borick S and Angell C A 2002 *J. Phys. Chem.* **106** 1069–80
       Velikov V, Lu Q and Angell C A 2003 at press

[10] Green J L, Ito K, Xu K and Angell C A 1999 *J. Phys. Chem.* B **103** 3991–6
       Bohmer R, Ngai K L, Angell C A and Plazek D J 1993 *J. Chem. Phys.* **99** 4201–9

[11] DeBolt M A, Easteal A J, Macedo P B and Moynihan C T 1976 *J. Am. Ceram. Soc.* **59** 16
       Moynihan C T 1976 *J. Am. Ceram. Soc.* **59** 16

[12] Phillips W A, Buchenau U, Nucker N, Dianoux A-J and Petry W 1989 *Phys. Rev. Lett.* **63** 2381–4

[13] Suck J B 1989 *Dynamics of Amorphous Materials (Springer Proc. Phys. vol 37)* ed D Richter, A J Dianoux, W Petry and J Teixera (Heidelberg: Springer) p 182
       Suck J B and Rudin H 1983 *Glassy metals II (Springer Topics in Applied Physics vol 53)* ed H Beck and H-J Güntherodt (New York: Springer) p 217

[14] Suck J-B 1993 *J. Non-Cryst. Solids* **153/154** 573–77
       Suck J-B 2002 *Adv. Solid State Phys.* **42** 393

[15] Wuttke J, Kriebel M, Bartsch E, Fujara F, Petry W and Sillescu H 1993 *Z. Phys.* B **91** 357

[16] Ambrus J H, Moynihan C T and Macedo P B 1972 *J. Phys. Chem.* **76** 3287

[17] Sciortino F, Kob W and Tartaglia P 1999 *Phys. Rev. Lett.* **83** 3214
       La Nave E, Mossa S and Sciortino F 2002 *Phys. Rev. Lett.* **88** 225701
       Mossa S, La Nave E, Stanley H E, Donati C, Sciortino F and Tartaglia P 2002 *Phys. Rev.* E **65** 041205
       Mossa S, La Nave E, Sciortino F and Tartaglia P 2003 *Eur. Phys. J.* B **30** 351

[18] Lewis L J and Wahnstrom G 1994 *Phys. Rev.* E **50** 3865

[19] Takeda K, Yamamuro O, Tsukushi I, Matsuo T and Suga H 1999 *J. Mol. Struct.* **479** 227–35

[20] Sastry S, Debenedetti P G and Stillinger F H 1998 *Nature* **393** 554

[21] Dyre J 1995 *Phys. Rev.* B **51** 12276

[22] Videa M and Angell C A 1999 *J. Phys. Chem.* B **103** 4185–90

[23] Franks F 1972 The properties of ice *Water: A Comprehensive Treatise* vol 1, ed F Franks (London: Plenum) pp 115–49

[24] Davy J G and Somorjai G A 1971 *J. Chem. Phys.* **55** 3624

[25] Richert R 2002 *J. Phys.: Condens. Matter* **14** R703–38
       Yang M and Richert R 2001 *J. Chem. Phys.* **115** 2676–80

[26] Reinsberg S A, Qiu X H, Wilhelm M, Spiess H W and Ediger M D 2001 *J. Chem. Phys.* **114** 7299
       Tracht U, Wilhelm M, Heuer A, Feng H, Schmidt-Rohr K and Spiess H W 1998 *Phys. Rev. Lett.* **81** 2727

[27] Cicerone M T and Ediger M D 1996 *J. Chem. Phys.* **100** 5237
       Ediger M D 2000 *Annu. Rev. Phys. Chem* **51** 99–128

[28] Bohmer R 1998 *Curr. Opin. Solid State Mater. Sci.* **3** 378

[29] Yue Y-Z *et al* 2003 at press

[30] Martinez L-M and Angell CA 2002 *Physica* A **314** 548
       Lin T C and Angell C A 1984 *Commun. Am. Ceram. Soc.* **67** C33

[31] Donth E 2002 *The Glass Transition* (Heidelberg: Springer) p 104

[32] Yue J-Z and Angell C A *Nature* (under review)

[33] Xia X and Wolynes P G 2000 *Proc. Natl Acad. Sci. USA* **97** 2990

[34] Tool A Q 1946 *J. Res. Natl Bur. Stand.* **37** 73
       Narayanaswamy O S 1971 *J. Am. Ceram. Soc.* **54** 491
       Moynihan C T *et al* 1976 *Ann. NY Acad. Sci.* **279** 15

[35] Kovacs A J, Aklonis J J, Hutchinson J M and Ramos A R 1979 *J. Polym. Sci. Polym. Phys. Edn* **17** 1097

[36] Hodge I M 1994 *J. Non-Cryst. Solids* **169** 211

[37] Hodge I M and Berens A R 1982 *Macromolecules* **15** 756

[38] Angell C A, Ngai K L, McKenna G B, McMillan P F and Martin S W 2000 *J. Appl. Phys.* **88** 3113–57
       See section D, and in particular figures 25 and 28

[39] Sokolov A P, Kisliuk A, Quitmann D, Kudlik A and Roessler E 1994 *J. Non-Cryst. Solids* **138** 172–4
       Engberg D, Wischnewski A, Buchenau U, Borjesson L, Dianoux A J, Sokolov A P and Torell L M 1998 *Phys. Rev.* B **58** 14

[40] Schroter K, Wilde G, Willnecker R, Weiss M, Samwer K and Donth E 1998 *Eur. Phys. J.* B **5** 1

[41] Vollmayr K, Kob W and Binder K 1996 *Phys. Rev.* B **54** 15808

[42] Soules T F 1979 *J. Chem. Phys.* **71** 4570
[43] Angell C A, Cheeseman P A and Tamaddon S 1982 *Science* **218** 885
[44] Vessal B, Greaves G N, Marten P T, Chadwick A V, Mole R and Houdewalters S 1992 *Nature* **356** 504
[45] Horbach J and Kob W 2002 *J. Phys.: Condens. Matter* **14** 9237
[46] Dederichs P H, Lehman C, Schober H R, Scholtz A and Zeller R 1978 *J. Nucl. Mater.* **69** 176
[47] Granato A V 1992 *Phys. Rev. Lett.* **68** 974
[48] Kob W, Sciortino F and Tartaglia P 2000 *Europhys. Lett.* **49** 590
[49] Sastry S 2001 *Nature* **409** 164
[50] Sastry S 2002 New kinds of phase transitions: transformations in disordered substances *Proc. NATO Advanced Research Workshop (Volga River, 2002)* ed V V Brazhkin, S V Buldyrev, V N Ryzhov and H E Stanley (Dordrecht: Kluwer) pp 589–601 see figure 4
[51] Khoshtariya D E, Dolidze T D, Lindqvcist-Reis P, Neubrand A and van Eldik R 2002 *J. Mol. Liq.* **96/97** 45–63
[52] Luck W A P and Ditter W 1969 *Z. Naturf.* B **24** 482–94
[53] Angell C A and Rodgers V 1984 *J. Chem. Phys.* **80** 6245–52
[54] Rahman A and Stillinger F H 1972 *J. Chem. Phys.* **57** 1281
[55] Mossa S, Matyushov D, Wang L-M and Angell C A 2003 in preparation
[56] Denny R A, Reichman D R and Bouchaud J-P 2003 *Phys. Rev. Lett.* at press
Denny R A, Reichman D R and Bouchaud J-P 2002 *Preprint* cond-mat/0209020
[57] Doliwa B and Heuer A 2003 *Phys. Rev.* E submitted
(Doliwa B and Heuer A 2002 *Preprint* cond-mat/0205283)
[58] Goldstein M 1976 *J. Chem. Phys.* **64** 4767
[59] Martinez L-M and Angell C A 2001 *Nature* **410** 663
[60] Angell C A, Richards B E and Velikov V 1999 *J. Phys.: Condens. Matter* **11** A75
[61] Angell C A and Borick S 2002 *J. Non-Cryst. Sol.* **307–310** 393
[62] Grigera T S, Martin-Mayor V, Parisi G and Verrocchio P 2003 *Preprint* cond-mat/0301103
[63] Parisi G 2003 *Preprint* cond-mat/0301284
[64] Reichmann D, private communication
[65] Muranaka M and Hiwatari Y 1995 *Phys. Rev.* E **51** R2735
[66] Perrera D N and Harrowell P 1999 *Phys. Rev.* E **59** 5721